ABSTRACT

Title of Thesis: NON DESTRUCTIVE EVALUATION OF CHLORIDE IN CONCRETE

Nafiseh Bozorgi-Fashand, Master of Science, 2011

Thesis directed by: Professor Amde M. Amde, Department of Civil and Environmental Engineering

Bridge decks in the cold climate region of the country, which have snow part of the year, are exposed to deicer salt in order to overcome the public demand for safe pavements. The chloride content in the salt can penetrate into the concrete through hairline cracks or diffusion in the concrete. This can establish galvanic corrosion microcells, and ultimately damage the concrete and reduce the life performance of the structure through expansive forces created by corroded steel. The issue of chloride penetrating into concrete has been under study and research for a long time. There is a critical need in civil engineering for methods that can nondestructively measure the condition of existing reinforced concrete structures. The focus of this thesis is on a nondestructive prompt gamma neutron activation (PGNA) chloride detector. This technique is a specialized use of prompt gamma/neutron activation, a spectroscopic technique for elemental analysis of materials. The elements of PGNA are identified by characteristic gamma rays emitted from the target material while it is being bombarded with neutrons. The objective of this research is to design a test program for determining the calibration factor, which relates the

detected chloride gamma ray counts to the actual chloride concentration in the concrete, and its uncertainties through the use of cast concrete samples with known chloride contents.

NON DESTRUCTIVE EVALUATION OF CHLORIDE IN CONCRETE

by
Nafiseh Bozorgi-Fashand

Thesis submitted to the Faculty of the Graduate School of the

University of Maryland, College Park, in partial fulfillment

of the requirements for the degree of

Master of Science

2011

Advisory Committee:
Professor Amde M. Amde, Chair
Professor Sherif Aggour
Professor Mohamad Al-Sheikhly

ACKNOWLEDGMENTS

First of all I thank my adviser, Professor Amde M. Amde for his support, supervision, and suggestions during the whole course of research.

Special thanks to Professor Richard Livingston, in the department of Materials Science & Engineering for his advice and guidance throughout the research.

I am very thankful to Dr. Jorgomai Ceesay, structural engineer at Greenhorne and O'Mara Consulting Engineers, for his technical support and assistance in concrete specimens preparation and analysis.

Thanks to Mr. Seth Rogge, graduate student at the civil engineering department at University of Maryland, for his assistance in concrete specimens' preparation.

Finally, I thank my family and friends for their encouragement, support and understanding.

Thank You.

TABLE OF CONTENTS

LIST OF TABLES

LIST OF FIGURES

1 CHAPTER ONE: INTRODUCTION

1.1 Problem Statement

The Federal Highway Administration reported that as of March 2011, there are approximately 600,000 bridges and overpasses in the United States. More than 11 percent of these bridges are structurally deficient (i.e. 70000). They also reported that 15 percent of the bridges are structurally deficient primarily due to corrosion of steel reinforcement caused by the deicing salt that penetrates into the structure (Goldmark, 2011). The corrosion of the bridge deck is a major cause of bridge deficiency. Bridge deck deterioration has been significantly increasing in the past decades due to two factors. First, the increased age of highway structures, and second, the "bare pavement" policy created by highway agencies in order to have safe roads in all weather conditions, has led bridges to deteriorate (Tonini & Dean, 1977).

Detecting corrosion of reinforcement in concrete at an early stage could help to save billions of dollars in the public and private budgets. Therefore, there is a critical need for a nondestructive test method that can detect chlorides in concrete to measure the condition of existing reinforced concrete structures (Goldmark, 2011).

When the salt in the deicing chemical reaches the reinforcing steel in the bridge deck, it causes the steel to corrode through an electrolytic process. A natural galvanic cell will be formed through steel corrosion. Chloride ions in the pore water forms the electrolyte and portion of the steel becomes the anode, and another portion becomes the cathode creating a macro corrosion cell. In a bridge deck there are different electrochemical cells, due to the fact that there will be

different chloride concentrations, oxygen availability and other factors. Corrosion causes expansion against the concrete cover. As a result, horizontal cracks develop along the upper plane of the steel causing delamination of the concrete. Potholes may also form as the traffic impacts the concrete above the fracture (Clear & Hey, 1973).

Ideally, the progress of chloride penetration into the concrete should be monitored frequently in order to predict the time of the corrosion. The deck of the bridge is the most exposed part of the structure in terms of penetrating chemicals and water. The corrosion of steel depends on both availability of oxygen and impairment of the protective oxide film. This oxide film is a result of atmospheric oxidation, which is a thin layer of iron oxide at the surface of the metal. As of today most applicable techniques that are utilized by highway agencies for monitoring chlorides are destructive and time consuming. Therefore, in this paper, a Nondestructive Evaluation Method that can detect chloride content in a structure is studied and tested. This method is a second generation Prompt Gamma Neutron Activation (PGNA) method that is under development at University of Maryland, College Park. The first generation PGNA had been previously developed by Federal Highway Administration (Livingston & Saleh, 2000). This system is essentially an improved version of the first generation.

In order to evaluate the performance of this system concrete specimens with known calcium chloride content were cast and tested. The objective of this project was to determine the calibration factor which is relationship between the detected chloride gamma ray counts and the actual chloride concentration in the concrete. In addition, research also had the goal of

determining the data quality parameters of sensitivity, precision, and minimum level of detection of the system.

1.2 Technical Approach

Prompt Gamma Neutron Activation (PGNA)

One way of approaching the problem of measuring chloride in concrete reinforcements is PGNA. In the past, this method has been used in various ways, such as oil exploration archaeology, and forensics. Recently, this technique is utilized to overcome the issue of conserving historical structures in Colonial Williamsburg and Venice, Italy (Livingston, 1993).

The PGNA method is a very critical method since its can detect the position of contaminants such as chloride (soluble salts) and water in the walls, deck of a bridge, or other parts of the structure. The system works by irradiating a section of a structure with neutrons from a portable source neutron such as the radioisotope ^{252}Cf. When the neutrons enter into the structure it is captured by the specific elements in the material which eventually generate gamma rays. Next, these characteristic energies (gamma rays) surpass the structure and are detected by a high-purity germanium gamma ray detector connected to a Multi-Channel Analysis (MCA) electronics module. This stores the number of counts of gamma rays in set of bins, or channels, each of which represent 1.3 keV of energy. Thus an MCA with 8192 channels can cover a gamma spectrum from zero to 10 MeV (Livingston & Saleh, 2000).

The MCA modules are now available in very compact package that can be plugged into a laptop computer. In the previous research it has been demonstrated that the neutron probe is feasible as a nondestructive method for measuring NaCl and H_2O contents of masonry (Livingston, 1993).

1.3 Outline of Report

This thesis consists of six chapters. Chapter one gives a brief review of the background and problem statement. Chapter two is a literature survey of the problems associated with chloride infusion into the reinforced concrete. The Chloride Threshold Levels are also discussed in this chapter along with the service life of concrete. In chapter three, Non Destructive Evaluation methods of detecting and monitoring the amount of chloride in concrete are discussed. Chapter four discusses the test methodology and the operating principle and conceptual design of the second generation PGNA, and specifications of chloride depth in the specimens. Chapter five discusses the laboratory specimens, describing the physical attributes of each concrete slab and tile cast at University of Maryland along with the calibration results of the concrete tiles that were taken to the Turner-Fairbank Highway Research Center. Finally, the summary and conclusions of this study are discussed in chapter six.

2 CHAPTER TWO: PROBLEM WITH CHLORIDE- LITERATURE SURVEY

2.1 Diffusion of Chloride into Concrete

The time to initiation of corrosion of the rebars, which is a result of chloride penetration into concrete, is a vital factor in determining the structure's service life. In order to determine the amount of chloride that has penetrated into the concrete, it is necessary to perform a chloride diffusion analysis. The corrosion of rebars starts when the amount of penetrating chloride into the concrete reaches a specific threshold level (Jang, et al., 2004). Chloride Threshold Values will be discussed further in Section 2.3 of this chapter.

2.1.1 The Relationship between Chloride Diffusion and Concrete Service Life

The estimation of the service life of reinforced concrete exposed to chlorides is based on a model of the diffusion of the de-icing salts as a function of time.

The calculation of the service life of the concrete depends on three factors:

$D_{eff,}$ which is the effective diffusion coefficient, and is mainly a function of concrete quality

C_o , which is effective surface concentration of the chloride, and depends on the level of concrete exposure to the environment, and can be influenced by concrete composition.

CTL, Threshold values of the chloride concentration that are needed for steel to corrode.

In designing reinforced concrete, chloride profiles are calculated based on different times using equation 2-1 (Laferriere, et al., 2008).

– **Equation 2-1**

Where,

C(x,t): the concentration C at the distance x, after time t

$C_{o:}$ concentration at boundary surface

erf: error function

Figure 2-1 illustrates the determination of the depth of concrete cover to achieve a specified service life, t, based on the calculated chloride profile (using D_{eff} for particular concrete and C_0 for the exposure conditions) at time t. The threshold values C_i and C_p are for corrosion initiation and corrosion damage. Cover depth D_i and D_p are the ones required for corrosion initiation and corrosion damage, respectively (Laferriere, et al., 2008).

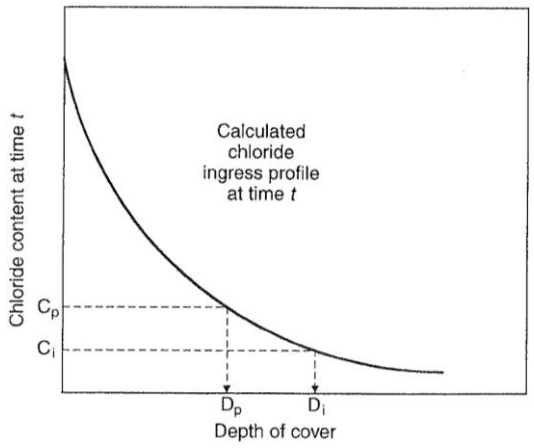

Figure 2-1- The schematic description of the determination of the depth of concrete cover to achieve specified service life, t, based on the calculated chloride profile

(Laferriere, et al., 2008)

2.2 Probabilistic Model for Chloride-Penetrated Corrosion in Reinforced Concrete

The model of diffusion represented by equation (2.2) is purely deterministic. However, actual field experience has shown that the service life has some stochastic aspects. This problem has been studied by Weyers et al.

Their probability model incorporates exposure to deicer salts and other known statistical factors that affect the corrosion process in order to determine when a bridge deck will need it first repair and when it can be expected to need subsequent maintenance. For this model created by Weyers et al, data was collected from 10 bridge decks built in Virginia. Data was obtained for surface chloride concentration, apparent diffusion coefficient, and clear cover depth. Analysis was done on several ranges of chloride corrosion initiation concentration, based on the existing research. In order to predict the time of first repair and subsequent rehabilitation, two re-sampling techniques were used – simple and parametric bootstrap techniques. Using these methods, all 10 bridge decks exhibited similar results. Data from several bridge decks in Virginia were utilized to integrate probabilistic deliberations into a service life model (Weyers, et al., 2002).

Water-cement ratio of 0.45, the clear cover depth of 2.5-3 inches, and other specifications that were used to construct these bridges were all the same. The specification requires a 28-day compressive strength of 27.6 MPa (4000 psi) which was used for the bridges.

Table 2-1- First time repair/rehabilitate of the bridges

(Weyers, et al., 2002)

Time to first repair and rehabilitation (in years)

$C_{(x,t)}$ from 0.6 to 1.2 kg/m^3

Structure no.	Parametric bootstrap			Simple bootstrap		
	% Corroded	2.5%	12%	% Corroded	2.5%	12%
1015	100	10	13	100	11	13
1004.3	100	23	31	100	23	30
1136	100	33	46	100	33	47
1001	100	28	48	100	28	49
1019	99	30	47	100	33	45
2262	96	31	56	91	34	52
2021	27	–	–	27	–	–
1004.6	19	–	–	18	–	–
6037	7	–	–	8	–	–
6128	0	–	–	0	–	–

The values listed in table 2-1 illustrate the estimated time for corrosion damage. These damages can be either spalling or cracking which happens after 4 years of exposure. The percent corroded column in the table corresponds to the number of model iterations in the simulation that predict corrosion damage in a bridge deck. The first time repair is shown with the 2.5 percentile column and the first time rehabilitation is illustrated with column 12 percentile values. The results of both the simple bootstrap and parametric bootstrap simulation were similar for all of the bridges (Weyers, et al., 2002).

Jang et al. state that in studying corrosion due to chloride penetration into concrete, the existence of rebars in the concrete have been greatly overlooked; which can adversely affect the corrosion penetration analysis. Jang et al. have done some studies in this matter to see the effects of steel bars on the chloride penetration, and furthermore, to establish the time of corrosion taking into

account the existence of rebars. They have also created models for chloride binding in concrete which assists the diffusion analysis. Variables such as rebar diameter, cover thickness of rebar, and water-cement ratio have been taken into account to study their effects on chloride diffusion (Jang, et al., 2004).

2.3 Chloride Threshold Levels

The definition for critical chloride content differs depending on the point of view from which one is examining critical chloride content. Scientifically speaking, critical chloride content is defined as the level of chloride needed for depassivation of steel. However, depassivation of steel does not always lead to deterioration. In dry concrete, for example, ohmic control of the current flow slows down the rate of corrosion. Therefore, from an engineering perspective, critical chloride content is defined rather as the chloride content present when visible or acceptable deterioration of a structure occurs. The differences in these two definitions are illustrated in Figure 2-2 (Angst & Venbesland, 2009).

The Degree of Corrosion model by Tuutli is compared to assumed constant chloride ingress, producing a linear increase in chloride concentration at the steel reinforcement. The two different models easily show how the critical chloride content differs depending upon which definition is being considered. Higher values are present in the “engineering definition”. Since more time is passes until the chloride content is determined, the definition 2 shows higher values (Angst & Venbesland, 2009).

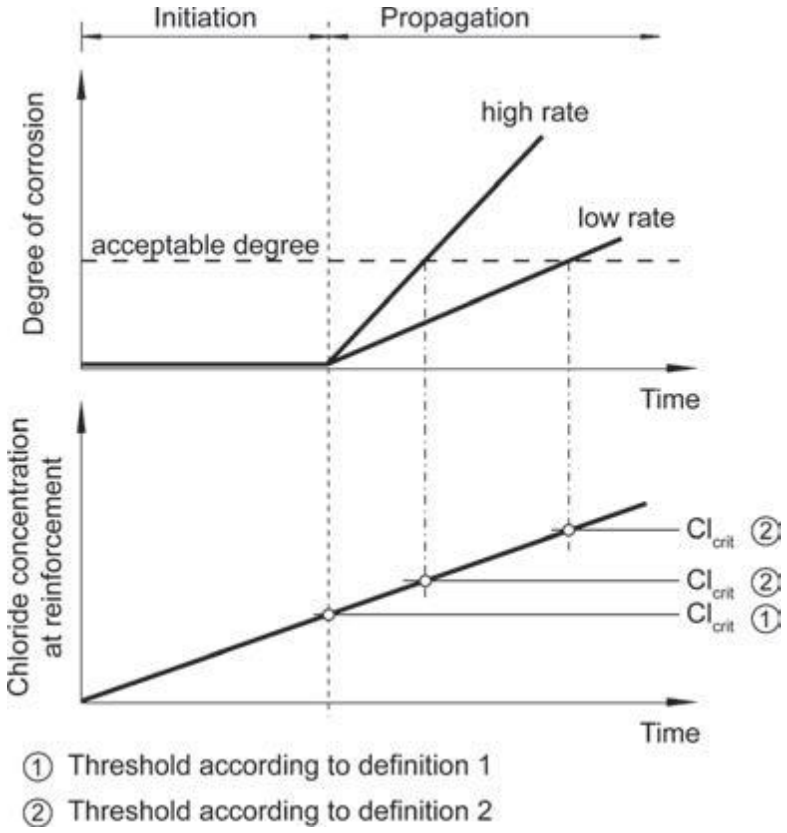

Figure 2-2- CTL definitions

(Angst & Venbesland, 2009)

Measurement of the total chloride content is fairly straight-forward using the destructive method of ASTM C-1152. However, this measures *total chloride content as weight percent of concrete*. However, the critical chloride threshold is usually expressed as *total chloride content relative to cement weight to eliminate variability due to binder/aggregate ratio*. In other instances, critical chloride content is expressed by use of free chloride contents related to the concrete weight, or as a concentration in mol/L in the pore solution. The reason for these different expressions of free chloride content is because the free chlorides are considered to be the most important for corrosion initiation (Angst & Venbesland, 2009).

Expressing critical chloride content solution as a CL-/OH – ratio stems from work done in solutions. The pH is crucial to this expression form as the CL-OH ratio will increase with a higher pH so that the inhibiting effect of OH becomes greater at higher pH levels. The CL-OH ratio expression has been widely regarded as the most reliable way to express critical chloride content. However, this notion has been challenged by some, notably Glass and Buenfeld who argue that critical chloride content is best expressed by the ratio of total chloride to binder weight. Based on the research the reported range of Chloride Threshold Values is 0.02 to 3.08% total Chloride by binder weight. However, American Concrete Institute (ACI 222R) guidelines suggests a range of 0.026% to 0.040% Chloride by mass of concrete. However, in general 0.05% by weight of concrete is practical (Angst & Venbesland, 2009).

3 CHAPTER THREE: NON DESTRUCTIVE EVALUATION METHODS-LITERATURE SURVEY

To date, no non-destructive method quantifying chloride content during the corrosion initiation phase has been established. Measurement of such a parameter is important for the development of a better understanding of the complexity of corrosion phenomena and, more practically, for better management of existing structures (Laferriere, et al., 2008). To evaluate the durability of reinforced concrete structures the measurement of the chloride content is necessary. Currently most of the methods to test chloride content are destructive. There are existing nondestructive methods but they are not widely utilized due to associated costs. The following section gives a brief synopsis of some of the current nondestructive methods.

3.1 X-Ray, Gamma Radiography Measurement

The quality of concrete along with defects can be identified using the Radiography technique which is another non-destructive method. This technique utilizes the radioactive isotopes for concrete and is a consistent method for identifying internal cracks, variations in density and voids. This technique falls into two categories of x-rays and γ rays. These two rays can pass through concrete and are not visible. They can be reduced based on density, thickness, and nature of material. This method works with the emission of photons by the radiation generator which is altered in visible light through a fluometallic converter in order to gain the ultimate reachable energy. Next, defects in concrete are identified through producing pictures. While using this technique safety should be the number one goal since radiation can be dangerous to people (Song & Saraswathy, 2007).

3.2 Half-Cell Potential

The overall condition of rebars and the likelihood of corrosion in reinforcements can be measured through Half-Cell Potential, which is another form of Non-Destructive Method. The ferric oxide protective layer around the concrete collapses when corrosion happens which tolerates an electrochemical reaction between concrete and rebars. The potential voltage difference in the concrete will be recorded utilizing a half-cell potential test when the reference electrode has exceeded the concrete surface. From the gauge reading, one can determine the location of corrosion and the possibility of corrosion occurrence. It is vital to monitor reinforced concrete frequently in order to identify signs, potentials, and severity of corrosion in reinforcements. This will help with forecasting the structure's service life and preventing immature failure (Pradhan & Bhattacharjee, 2009).

Detecting the severity of corrosion in steel can be done through measuring the corrosion potential due to the fact that it is qualitatively related to the reinforcement's corrosion rate. The potential difference between a standard portable half-cell, which is usually a copper/ copper sulphate (Cu/CuSO4) can be measured with a standard reference electrode by placing it on the surface of the concrete while keeping the reinforcement beneath. This is done by injecting water into a hole of approximately 5 mm diameter that is bored over the asphalt coating (Figure3-1) (Rhazi, 2001). The schematic basic of the half-cell potential illustrated in Figure 3-2 shows that the positive end of the voltmeter is connected to the reference electrode, while the negative is attached to the reinforcement.

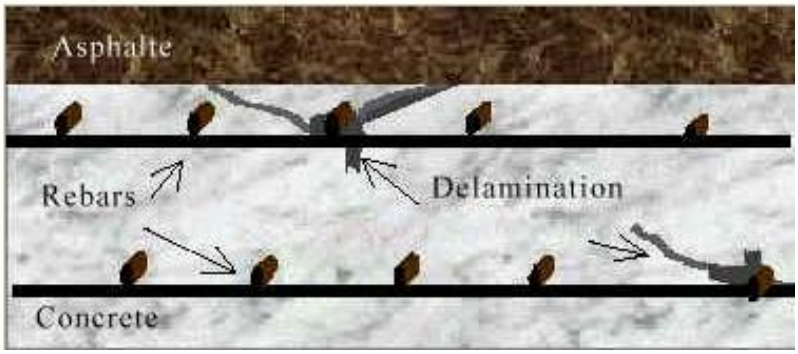

Figure 3-1- half-cell potential

(Rhazi, 2001)

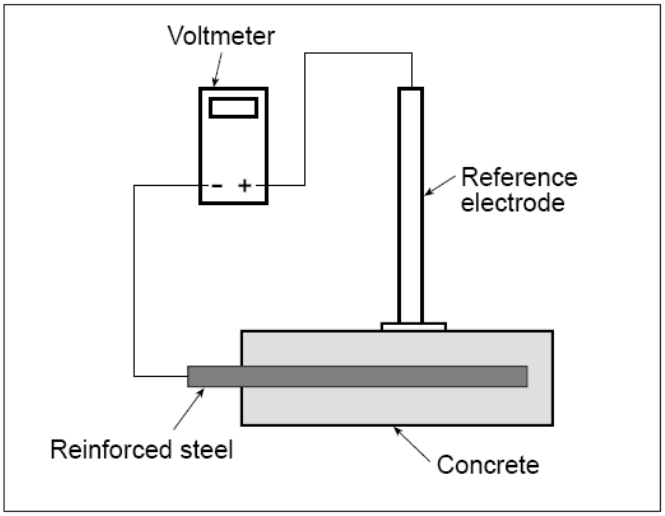

Figure 3-2- Schematic showing basics of the half-cell potential

(Rhazi, 2001)

The degree of corrosion within the reinforcement and the adjacent concrete can be measured by utilizing half-cell potential test. ASTM C876-80 which is called the "Standard Test Method for Half-Cell Potentials of Reinforcing Steel in Concrete" explains this method in depth.

In order to measure the corrosion in rebars, a 1m x 1m size grid pattern is employed to detect places where the half-cell is to be located on bridge decks. Next, the gathered data is plotted on schematic diagrams of the bridge as an equipotential contour map. Based on the ASTM standard, if the potential is greater than -200 mV, the probability of corrosion is less than 10%. However, a high probability (>90% which is active corrosion) is present if the potential value is lower than -350 mV. The corrosion activity is unclear if the values are between these two limits (Rhazi, 2001).

3.3 Ground Penetrating Radar (GPR)

This technique has many characteristics in common with the acoustic sonar technique. GPR uses a high frequency electromagnetic wave, which is normally between 1 GHz to 2.5 GHz. Under careful evaluations, this wave is emitted by an antenna into the concrete. Next, a receiver antenna detects, records, and analyzes the reflected energy that is the result of the electromagnetic properties of the material. This phenomenon is illustrated by a graph in Figure 3-3 (Rhazi, 2001).

In general this method utilizes air-coupled horn antennas or ground-coupled antennas that are placed from 0.3 to 0.5 meters above the deck surface. The reinforcing steel can be presented as a continuous layer when using the horn-antenna since it detects several rebars at the same time. In addition, the ground-coupled antenna has the capability to differentiate each bar due to its nearness to the bar (Rhazi, 2001).

It should be noted that the contemporary Ground Penetrating Radar has the ability to gather radar waveforms at a rate of more than 100 per second. Therefore, the data can be gathered at driving speeds. Using a distance transducer which is connected to the drive train of the vehicle that is

gathering the data, the horizontal positioning of the data can be achieved. The whole surface of the deck can be covered by varying the location of the antennas across the width of the deck (Rhazi, 2001).

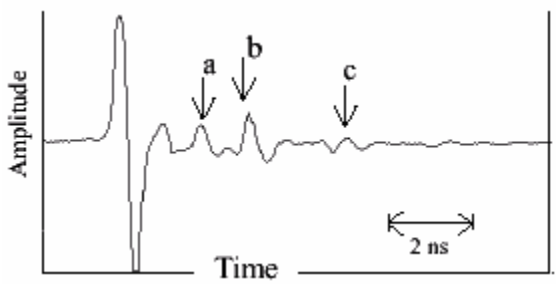

Figure 3-3- Typical GPR waveform showing the reflection at (a) the asphalt-concrete interface, (b) top rebar and, (c) bottom rebar

(Rhazi, 2001)

The conductivity of the concrete increases as the chloride content and the moisture does. At locations where attenuation was greater than -12.5 dB, the GPR results were the same as the manual sounding result. The manual sounding has made it easier for the researchers to identify the corresponding value of the attenuation that relates to the border between deteriorated concrete and sound concrete. This is due to the differences in site conditions that cause a wide range of threshold that cannot be applied to all sites (Rhazi, 2001).

In the past, the research involved in GPR analysis was not conclusive but rather, it was subjective due to the following facts; first, it elaborated the waveforms of the echo persuaded by the presence of delamination. Second, it did not produce definite results even at 2.5 GHz due to the radar wavelength in concrete being too large to resolve the 1-2 mm delamination cracks (Manning & Maslewic, 1990).

Different GPR data studies undergone in the early 1990's investigated the causes of delamination instead of investigating the delamination itself. These approaches were not very effective since it was difficult to interpret the resulting data. These studies basically relied on changing the concrete's moisture and chloride contents that cause deterioration (Huston, et al., 1996) & (Cady & Gannon, 1992).

3.4 The Infrared Thermography

The delaminated areas of a bridge heat faster under the suns infrared rays due to the fact that the present fracture on the surface stands in as an insulator and receives all the heat close to surface. These spots on the deck are usually about 2-5 degree Celsius hotter than any other area on the deck (Manning & Maslewic, 1990) and can be identified by an infrared camera. This detecting method is described in ASTM D4788 *"Test method for detecting delaminations in bridge decks using infrared thermography".*

This method works by a vehicle and equipment that are driven on the bridge deck under investigation at a speed of 16 km/hr. Then, the infrared data can be detected and gathered and images are recorded on a video tape. The outcome of this technique is a map that shows all the areas of the bridge that have been delaminated due to chloride penetrating into the reinforced concrete. The delamination can be shown as a white, or hot, area in the nearby black, or cooler, background (Manning & Maslewic, 1990).

This technique is highly interesting for DOT agencies since it can test a specific area of a deck. Also, analyzing the gathered data is simple and can be done in real time. Nonetheless, the efficiency of this method depends on the surrounding environment and the condition that the

deck is in. One of the down sides of this method is that the depth of the damage cannot be identified. Therefore, it is unlikely to determine whether the subsurface void is close to the surface or not at the asphalt-concrete boundary or beyond the level of rebars. Moreover, as the asphalt coating increases, the determination of the method decreases. This technique is more useful when combined with the Ground Penetrating Radar method since both techniques together increase the reliability of evaluating the condition of the deck (Manning & Maslewic, 1990).

3.5 First Generation Neutron-Based System, PGNA

A portable system for detecting chlorides in concrete has been previously developed using prompt gamma neutron activation (PGNA) based on a ^{252}Cf neutron source. In PGNA, neutrons are captured by nuclei in the target and gamma-rays of characteristic energy are emitted.

A number of elements can be detected depending on the neutron capture cross section and the gamma-ray yield. The reaction ^{35}Cl (n, γ) ^{36}Cl is especially useful because of its large neutron capture cross-section, 33.2 barns and also because of the emission of several gamma rays covering a wide range of energies (Livingston, 1993).

A schematic diagram of the existing chloride detection system is given in Figure 3-4. The ^{252}Cf radioisotope neutron source generates fast neutrons with typical energies in the 1-5 MeV range, while PGNA requires thermal neutrons (2.57×10^{-8} MeV). Therefore it is necessary to use a polyethylene moderator to slow down the neutrons to thermal energies. These thermalized neutrons enter the concrete and are captured by various nuclei including Cl. The gamma rays emitted during capture are then detected by High Purity Germanium (HPGe) coaxial type.

However, the HPGe detector essentially detects gamma rays coming from any direction. This omnidirectional operation leaves some room for improvement.

The sampled volume in the concrete is relatively large ~100,000 cm3 so that the spatial resolution is relatively coarse. The chloride signal is averaged over depth, so it is not possible to measure the depth profile, which is important to assessing possible corrosion risk. The detector is sensitive to gamma rays generated by the hydrogen content of the moderator around the source, which makes it impossible to measure water within the concrete itself, which is an important parameter. The detector is also sensitive to the gamma-rays produced by PGNA of other elements in the moderator which adds significant background. To overcome these drawbacks, a second-generation PGNA chloride measurement based on an electronic collimator is being developed and evaluated (Livingston, 1993).

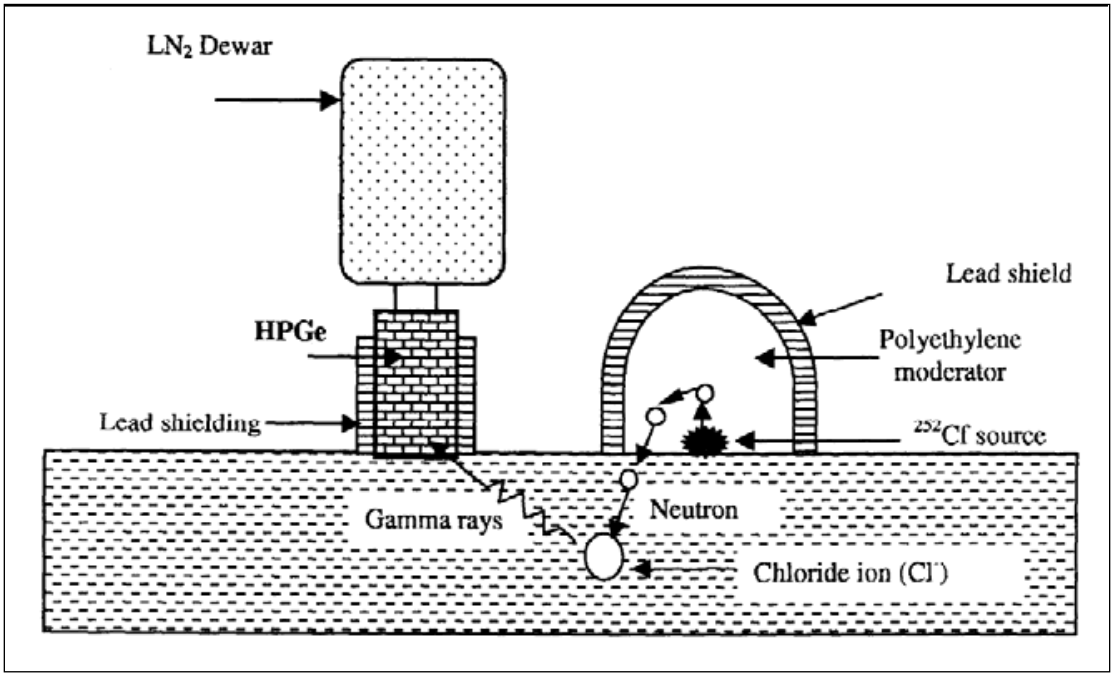

Figure 3-4- First generation PGNA

(Livingston, 1993)

4 CHAPTER FOUR: TEST METHODOLOGY

4.1 Second Generation Neutron-Based System, PGNA for Measuring Chloride in Concrete

An improved version of the PGNA system is now in development which makes use of an electronic collimator subsystem to improve directionality and reduce background. It incorporates a second thin sodium iodide (NaI) detector in front of the main high purity germanium (HPGe) detector which measures gamma-ray energies with high resolution. The associated electronics enable counting in the coincidence mode so that only gamma-rays that first pass through the NaI detector are then analyzed by the HPGe detector. This limits the field of view of the system to approximately the area of the NaI detector which can be as small as 1 cm^2. Depending on the material composition, the depth of penetration can be tens of cm. In order to compensate for the lower count rate caused by the introduction of the second detector, a deuterium-tritium (D-T) fusion neutron generator will be used instead of the ^{252}Cf radioisotope neutron source. In addition to providing a more intense neutron current, about 30 times greater, the use of the neutron generator would minimize the need for radiation shielding during transport (Livingston, et al.(TRB), 2010).

4.1.1 Numerical Simulation of the PGNA Signal from Chlorine Diffusion Gradients in Concrete

The performance of PGNA has been previously modeled using a hybrid MCNP/optical ray tracing approach. The chloride concentration has a non-linear depth profile which is typically modeled by the erfc function due to the fact that the chlorides are the result of de-icing salts

applied to the concrete surface. Since the chloride ion is a vital promoter of the corrosion of iron reinforcements in concrete, a portable nondestructive method for testing the chloride content has been developed based on prompt gamma neutron activation (PGNA). This system involves an HPGe gamma ray detector, a ^{252}Cf neutron contained in a polyethylene moderator, and supplementary electronics such as laptop etc. In the past study (Livingston, et al. (TRB), 2011).

This method was utilizing a hybrid MCNP/optical ray tracing approach to calculate the 6.111MeV signal. This signal is essentially the integral over the sample volume of nearly 100,000cm^3. A spatially uniform Chloride distribution was assumed for this method which is not always the case since the chlorides that build up due to the de-icing salts applied to the concrete surface lead to a non-uniform distribution which also changes over time. The chloride concentration is in fact non-linear and can be demonstrated by the Fick's Law diffusion gradient using the erfc function.

—— Equation 4-1

Where c(x) is the Cl concentration at depth x, c_s is the concentration at surface and D is the diffusion coefficient (Kirkpatrick et al., 2002; Thomas, 2001).

4.1.2 Specification of Cl Depth Profiles

Using equation 4-1 and given a value or D, chloride depth profiles can be generated as illustrated in Figure 4-1. The most applicable units for D are in cm^2/yr that is 1.577cm^2/yr(Livingston, et al.(TRB), 2011).

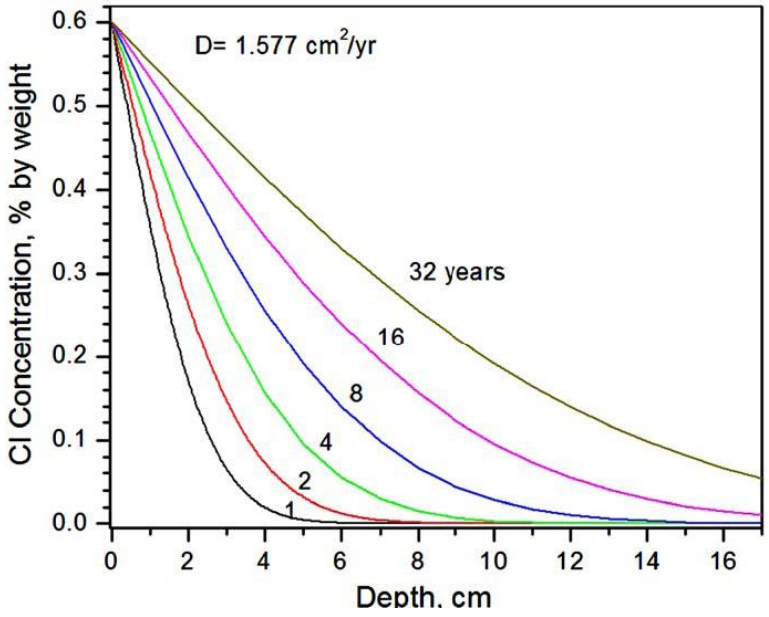

Figure 4-1- Evolution of Chloride depth profile as a function of time

(Livingston, et al.(TRB), 2011)

It is important to specify a threshold value for chloride concentration in concrete if the curves shown in Figure 4-1 are being applied. The threshold phenomenon is a provocative matter, but usually it is 0.05% by weight of concrete. Considering Figure 4-1, for instance, a reinforced concrete that has a depth of 7.5 cm, will have active corrosion between 4 to8 years. However, severe damage in the structure does not begin until several years of exposure to chloride (Livingston, et al.(TRB), 2011).

4.1.3 Conceptual Design of Second Generation System

The first generation system is omni-directional and thus samples a very large volume. In order to improve the spatial resolution, it is necessary to make the detector more directional by introducing a collimator to constrain the solid angle in which the gamma-rays are detected. In the laboratory this is usually done by a physical collimator, which consists of a shield of dense

material such as lead around the detector, with an opening that defines the direction. However, the thickness of lead required to attenuate a 6.111 MeV gamma ray coming in the wrong direction by a factor of 100 would be about 10 cm. Consequently, the mass of the entire collimator would be about 250 lbs, which would be impractical for a system intended to be portable. An alternative approach employed here uses an electronic collimator based on the Compton telescope configuration (Livingston, et al.(TRB), 2011).

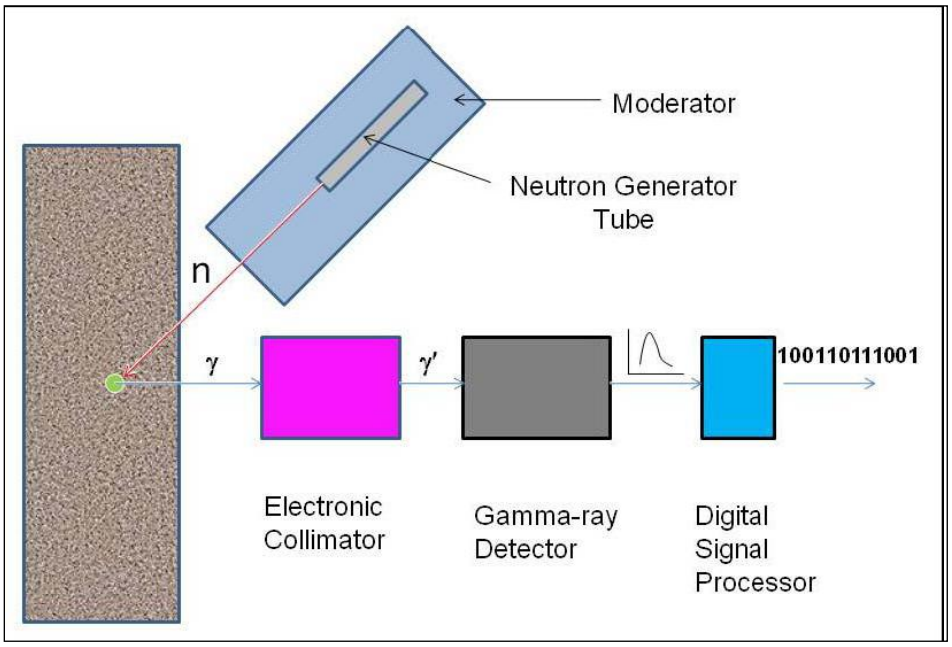

Figure 4-2- Conceptual design of 2nd generation chloride measurement system

(Livingston, et al.(TRB), 2011)

In this system, a gamma-ray emitted from the concrete first passes through the electronic collimator. If it is traveling in the right direction, i.e. from the concrete, it is counted. In the process, the gamma-ray gives up a small amount of energy through Compton scattering. The gamma-ray leaving the collimator then enters a conventional HPGe detector where its remaining energy is measured. The output of the HPGe detector is an analog voltage pulse as shown in

Figure 4-2. In conventional counting electronics, this pulse is integrated to give a total charge, which is then digitized for assignment to a specific counting bin or channel. In the 2nd generation system, another innovation is the introduction of a digital signal processor that digitizes the actual shape of the analog pulse. This enables more precise determination of the gamma-ray particle's energy. The third innovation is the replacement of the ^{252}Cf radioisotope source by a neutron generator. This is motivated by the fact, as discussed below that introducing the electronic collimator reduces the overall count rate. Commercially available portable neutron generators use the deuterium-deuterium (D-D) or deuterium-tritium (D-T) fusion reaction to generate the neutrons and can produce neutron currents as high as 3x108 n/s, which is about 30 times greater than the maximum from the ^{252}Cf radioisotope source. In addition to providing a higher neutron flux, the use of the neutron generator would minimize the need for shielding requirements during transport (Livingston, et al.(TRB), 2011).

In addition to the improved spatial resolution of the detector, background would be significantly reduced, thereby improving the counting statistics and reducing the time required to make a scan of an area. By eliminating the hydrogen signal from the moderator, it would also be possible to measure the water/cement ratio in the concrete. Also, the neutron generator can be operated in a pulsed mode. This makes it possible to measure additional elements by fast neutron activation and also to make time-of-flight measurements for depth profile measurement (Livingston, et al.(TRB), 2011).

4.1.4 Design of the Electronic Collimator

As discussed above the electronic consists of a very thin planar detector mounted in front of the existing coaxial HPGE detector as shown in Figure4-3. A gamma-ray photon traveling in the preferred direction enters the front of the first detector and gives up a very small amount of energy by Compton scattering, which involves knocking loose an electron. This event is detected and starts the timing circuit. The photon then exits the first detector and enters the HPGe detector where the rest of its energy is deposited. The two detectors would operate in coincidence mode, so that only the gamma-rays passing through both within a specified time window would be counted, and those from other directions would be rejected (Livingston, et al.(TRB), 2011).

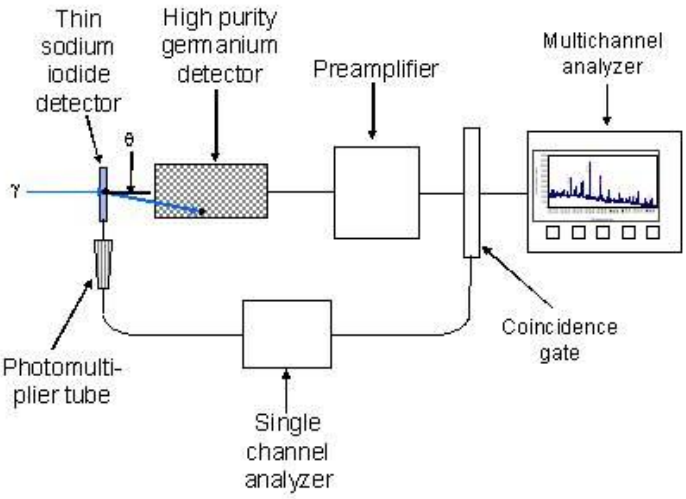

Figure 4-3- Schematic diagram of the electronic collimation system

(Livingston, et al.(TRB), 2011)

As shown in Figure 4-3 the Compton-scattered photon moves off in a direction that is at an angle θ to the incident direction. If this angle is too large the photon will miss the HPGe detector entirely and thus not be counted. The limiting value of the angle is clearly:

– Equation 4-2

where r is the radius of the HPGe detector and *s* is the separation between the two detectors. The radius is fixed at 3.8 cm, but *s* is adjustable.

The angle θ is related to the energy given up in the scattering event. The angle can be calculated from the Klein-Nishina relationship which is simply the conservation of energy modified to take into account relativistic effects:

Equation 4-3

Where ν the wavelength of the incident gamma-ray, h is Plancks's constant and $m_o c^2$ is the rest mass energy of the electron (0.512 MeV). The maximum detectable energy loss occurs when $\theta \approx 90^{\circ}$, since at higher angles the photon is backscattered and does not enter the HPGe detector. For the 6.111 MeV chloride photon, this maximum energy loss would be 5.610 MeV or about 92%. The scattered photon would thus have energy of 0.501 MeV.

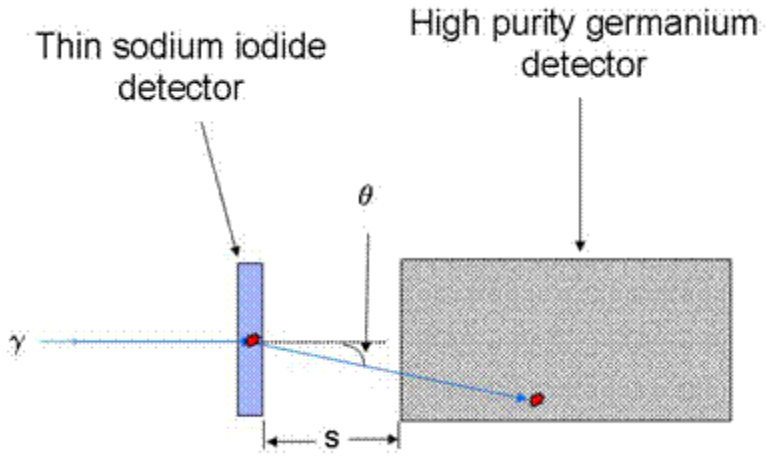

Figure 4-4- Geometry of Compton Scattering

(Livingston, et al.(TRB), 2011)

The probability of scattering into a specific angle θ is given by the Klein-Nishina relationship which indicates that at 6.111MeV, the distribution would be highly peaked in the forward direction and hence the typical value of θ would be very low. On the other hand, the photon has to deposit a certain amount of energy above the minimum detectable in the first detector for it to be detected. If it is not detected then the time window will not be opened. The minimum detectable energy depends on the material and geometry of the first detector and the noise level of the associated electronics. Thus the performance of the systems has to be determined by a combination of numerical simulations and empirical calibrations (Livingston, et al., 2011).

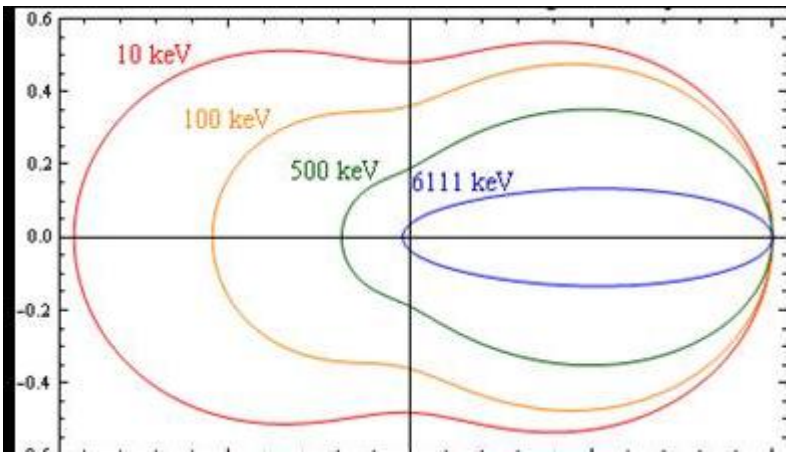

Figure 4-5- Angular distribution of scattering photons

(Livingston, et al.(TRB), 2011)

In addition to the detector separation, *s*, another important parameter in the design of the electronic collimator is the thickness of the NaI detector. An incident photon has to have at least one scattering event in the detector in order to start the counting process. Thus the probability of such an event, p_{scat}, should be as large as possible. This given by:

– Equation 4-4

Where I_o is the incident beam intensity, I is the intensity at the distance x into the material, and λ is the mean free path, i.e. the average distance a photon travels before a scattering (or absorption) event (Livingston, et al.(TRB), 2011).

This implies that the ratio x/λ should be as large possible. The mean free path is a property of the material, and is thus fixed. Consequently, the only way to increase the ratio is to increase x, which in this case is the thickness of the NaI detector. However, as the detector becomes thicker,

the probability increases of a photon entering it from the side instead of the front and thus triggering a false count (Livingston, et al.(TRB), 2011).

The mean free path is a function of the photon energy. The result is that for a 6111 keV photon in NAI, $\lambda = 7.81$ cm. Consequently, for a 2 cm thick detector the probability of a triggering event is about 0.23. Thus, inserting this second detector before the HPGe detector would reduce the count rate by a factor of roughly 5. If this is unacceptable, it is possible to compensate for this reduction in several ways including increasing the neutron source strength or going to a lower energy gamma-ray emitted in the PGNA of chlorine, which would have both a shorter mean free path and a higher detection efficiency in the HPGe.

The resulting design of the NaI detector is presented in the drawing in Figure 4-6. This configuration with the photomultiplier tube (PMT) co-planar with the NaI disk is known as a "banjo" detector. It may be desirable in the future to turn the PMT 90º, i.e. parallel to the axis of the disk, to make the overall chloride measurement system more compact. This can be done by inserting a prism at the window between the NaI disk and the PMT. However, this would result in some loss of signal (Livingston, et al., 2010).

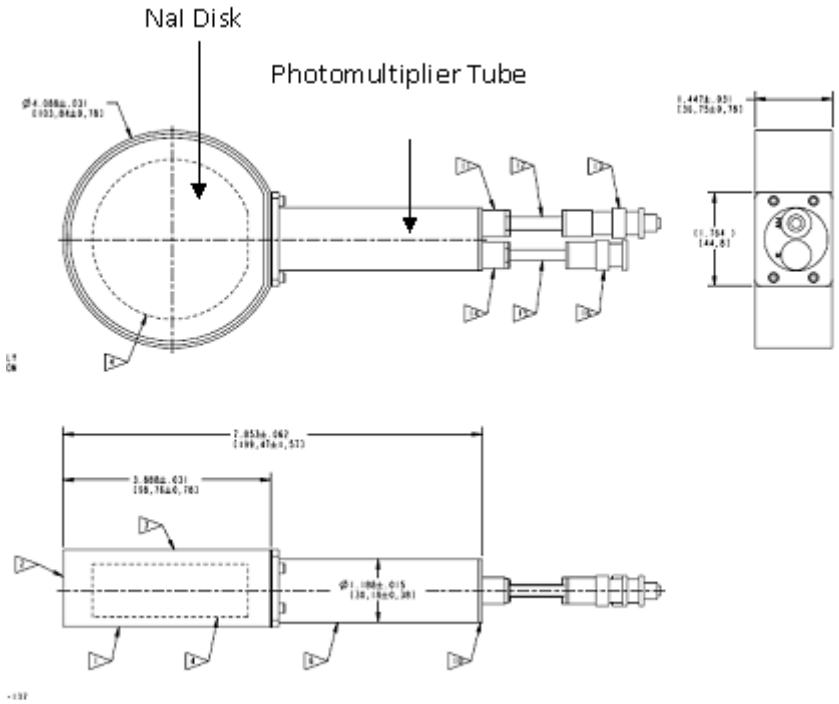

Figure 4-6- Design of the NaI detector

Dimensions are in cm
(Livingston, et al. (TRB), 2011)

4.1.5 Neutron Generator

As discussed above, the introduction of the NaI detector reduces the counting rate. To compensate for this, the ^{252}Cf radioisotope source is replaced by a neutron generator which can give a higher neutron flux. It is actually a compact linear accelerator. The ion source is deuterium gas. The deuterons are stripped of electrons which gives them a positive charge. They are then accelerated by the large voltage difference between the ion source and the target. When the accelerated deuterons hit the target which can be either more deuterium (D-D) or tritium (D-T) fusion happens with the production of a helium atom and a neutron. This appears to be a highly complicated system that would be difficult to operate in the field, but in fact,

commercial systems based on sealed tube design have been developed. These are simple to use and reliable. Consequently, they are now used in a number of applications in the field, such as petroleum detection and explosives detection (Livingston, et al.(TRB), 2011).

The main issue for the specification of the neutron generator is the selection of the type (D-D or D-T) of neutron generator tube. One consideration is the energy of the neutrons. The D-T fusion reaction produces a 14.1MeV neutron. The D-D reaction produces a lower energy neutron with 2.45 MeV. In comparison, ^{252}Cf emits neutrons with a range of energies with the most probable value being about 2 MeV. Thus a larger volume of moderator than currently used would be required to slow the neutrons down to thermal energies. This would increase the bulk and weight of the overall system. On the basis of neutron energies it would appear that D-D type would be preferable since the neutron energies are relatively close to that of ^{252}Cf. The neutron source strength must also be considered. The D-D nominal yield is 2.5×10^6 n/s while the D-T yield is 3.0×10^8 n/s. Thus the D-D system would produce fewer neutrons than the existing ^{252}Cf source. Therefore the choice is the D-T system (Livingston, et al.(TRB), 2011).

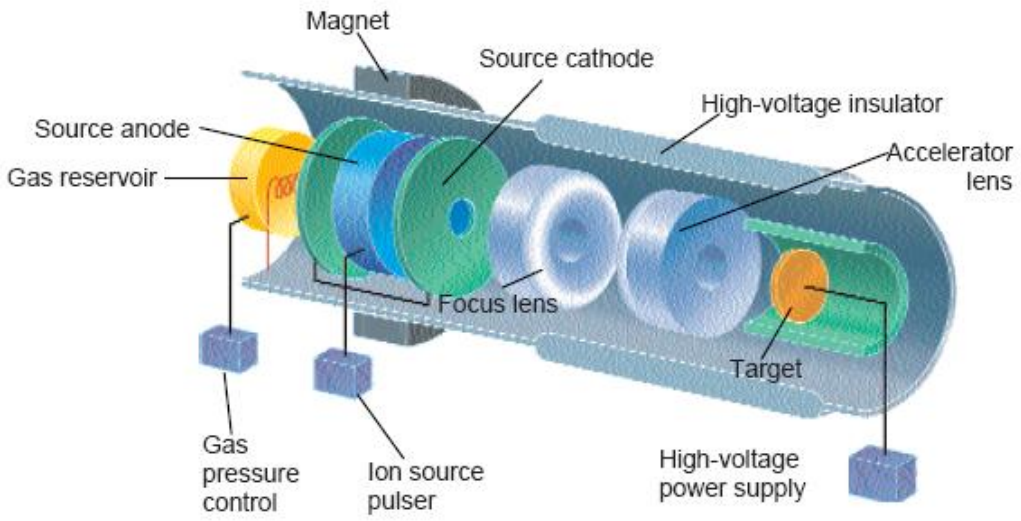

Figure 4-7- Schematic diagram of the compact portable neutron generator

(Livingston, et al.(TRB), 2011).

4.1.6 Moderator Design

The replacement of the ^{252}Cf radioisotope neutron source with the D-T neutron generator requires a re-consideration of the design of the moderator for two reasons. One is the difference in geometry between the two sources. The ^{252}Cf comes in a cylindrical capsule 0.5 cm in diameter by 2.5 cm length, while the D-T tube is 20 cm in diameter and 70 cm in length. The other is the difference in the energy of the emitted neutron, ~ 2 MeV for the ^{252}Cf vs 14.1 MeV for the D-T tube, which implies that the moderator for the latter would need more volume to slow the fast neutrons down to thermal velocity.

Moderator design for field applications is not yet an exact science. Ideally, the moderator should maximize the delivery of thermal neutrons to the target while minimizing losses due to capture,

and at the same time minimizing the radiation exposure to the operators (Livingston, et al., 2011).

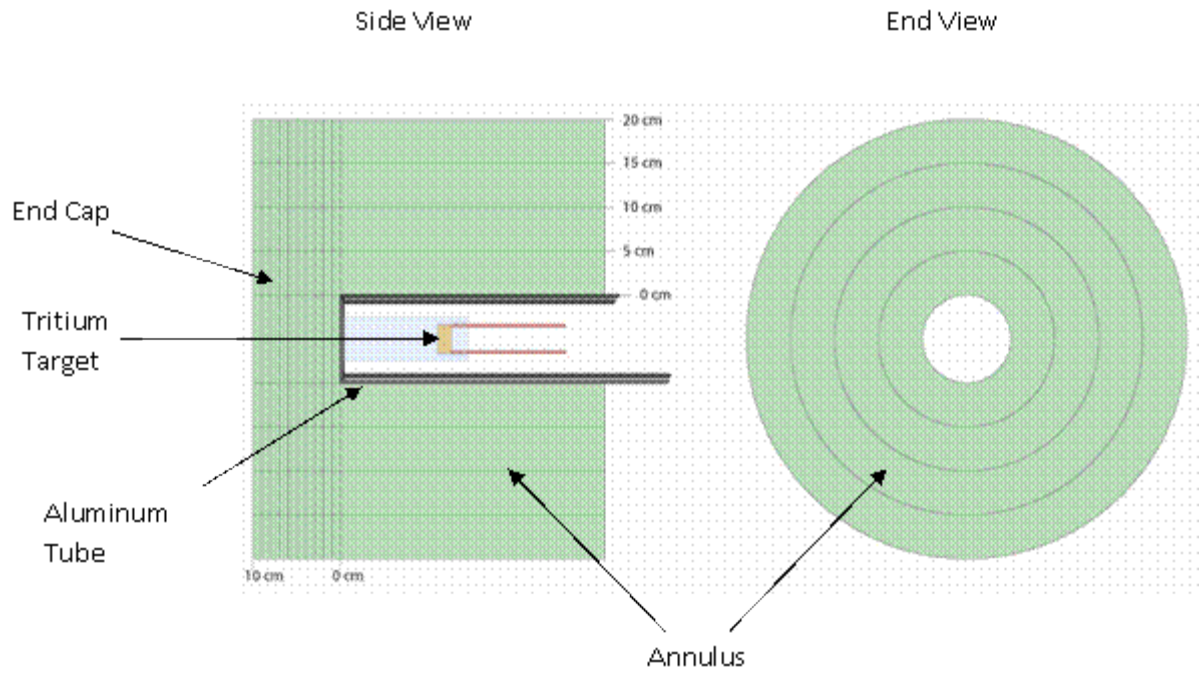

Figure 4-8-Schematic diagram of moderator geometry for the D-T tube

(Livingston, et al.(TRB), 2011).

The moderator design used in the first generation PGNA system consisted of a solid cylinder of polyethylene 15 cm in radius with a hemispherical end cap. The preliminary design for the D-T tube (Figure 4-8) consists of a cylindrical annulus into which the tube fits, and a end cap between the face of the tube. The material chosen for the moderator is polyethylene. This contains a significant amount of hydrogen, which is the most efficient element for neutron scattering and thus the most effective at slowing down the neutrons. However, it also has a large cross-section for absorption. Consequently, the thermal neutron flux in the moderator is the balance between two competing processes: slowing down of fast neutrons, which increases the thermal neutron

population and absorption, which removes them. This problem can't be solved analytically. Therefore, it has to be modeled by numerical simulations using the computer software MCNP (Livingston, et al.(TRB), 2011).

The effect of varying the dimensions of the moderator shown in Figure 4-8 was thus investigated by MCNP computer simulations. Five different values for the annulus wall thickness ranging 0-20 cm were chosen. For each of these thicknesses, the thickness of the end cap was varied systematically from 0 to 10 cm in 1 cm increments. The results are presented in the plots in Figure 4-9. The thermal neutron flux for the point at center of end face is plotted against the end cap thickness. It can be seen that for the end cap by itself without an annulus, the flux peaks at a value of 615 n/cm^2s. Any additional thickness tends to act slightly more as an absorber than a moderator (Livingston, et al.(TRB), 2011).

Adding an annulus significantly increases the thermal neutron flux by nearly an order of magnitude. One reason for this is that neutrons that travel in the radial direction, and would otherwise be lost, are scattered into the axial direction. It can be seen there is no significant increase the neutron flux going from a wall thickness of 15 cm to 20 cm. This increment of thickness would increase the overall weight of the moderator by 38%. This suggests that the optimum wall thickness would be 10-15 cm. Finally, for any wall thickness, adding a thin end cap causes an actual decrease in neutron flux. It then reaches a local maximum for an end cap thickness around 3 cm (Livingston, et al., 2011).

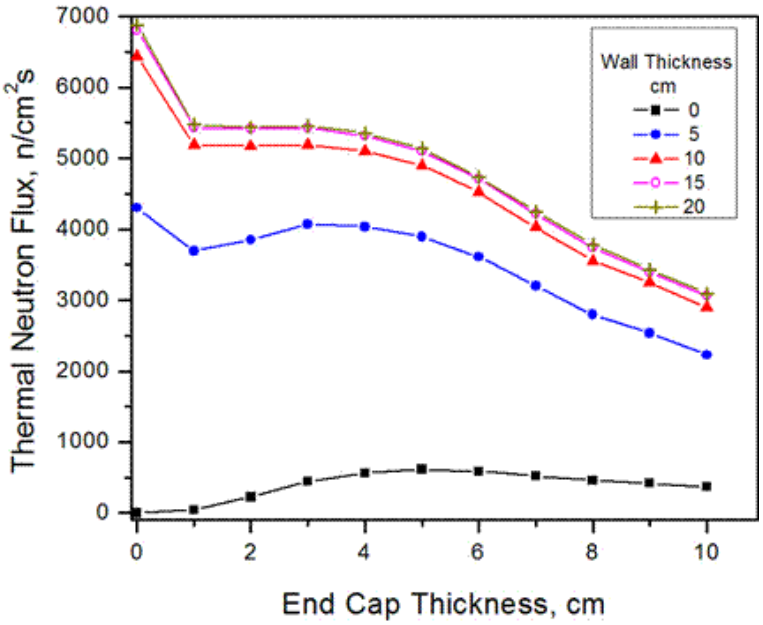

Figure 4-9- Thermal neutron flux at center of moderator end face

(Livingston, et al.(TRB), 2011)

5 CHAPTER FIVE: LABORATORY SPECIMENS

The objective of the PGNA test is to come up with a quantitative measurement technique. We will have to present the data quality parameters based on the calibration of the system on the concrete slabs. The key parameters which are the non-destructive statistical considerations are accuracy, sensitivity, reliability, which consists of probability of detection and false positive, and lastly minimum of detection. In order to evaluate the performance of the system, it is necessary to have test specimens with known chloride contents. Therefore, specimens are being cast with calcium chloride added to the mix water of the concrete batches in specified amounts.

5.1 Aggregate Selection

The maximum size of the coarse aggregate was limited by the requirement of casting concrete tiles with a thickness of 1', as discussed below. The coarse aggregate was silicate river gravel and the fine aggregate was silicate sand from Chaney Enterprises in Waldorf Maryland.

Table 5-1summarizes the analysis aggregates used to cast the concrete specimens. The first column is the sieve size and sieve number, and the second column is the accumulative percent passing.

Table 5-1- Aggregate Analysis

Type of Material: ASTM C-33 #8 Gravel		**Type of Material: ASTM C-33 & C-404 Fine Aggregate**	
SIEVE SIZE/NUMBER	**CUMULATIVE PERCENT PASSING**	**SIEVE SIZE/NUMBER**	**CUMULATIVE PERCENT PASSING**
3 inch		3 inch	
2 ½ inch		2 ½ inch	
1 ½ inch		1 ½ inch	
1 inch		1 inch	
¾ inch		¾ inch	
½ inch	100	½ inch	
3/8 inch	90.6	3/8 inch	100
#4	16.6	#4	98.5
#8	0.8	#8	82.8
#16	0.3	#16	59.3
#30		#30	44.8
#50		#50	15.8
#100		#100	2.1
#200		#200	0.1

Dry Rodded Unit Weight PCF	98.7	Dry Rodded Unit Weight PCF	104.1
Organic Impurities		Organic Impurities	Plate 1
Fitness Modulus		Fitness Modulus	2.97
Bulk Specific Gravity S.S.D	2.53	Bulk Specific Gravity S.S.D	2.6
L.A. Abrasions, Grading (B), Percent Loss by Weight	33.2	L.A. Abrasions, Grading (B), Percent Loss by Weight	
Soundless(Magnesium Sulfate), Percent loss by Weight	3.9	Soundless(Magnesium Sulfate), Percent loss by Weight	4.80%
Flat and Elongated (percent by Weight)		Flat and Elongated (percent by Weight)	
Clay lumps and friable Particles	0.7	Clay lumps and friable Particles	0%
Absorption	1.20%	Absorption	0.7
Soft particles		Soft particles	
Light weight pieces (Floating)	0.00%	Light weight pieces (Floating)	0.00%

5.2 Description of the Concrete Specimens

5.2.1 Slabs

The concrete specimens were cast using weight percent by concrete mass obtained using the current destructive AASHTO T260 method. This can be converted to weight percent by cement. The first specimen type is a slab with dimensions of 3ft by 3ft by 5 inches (90 x 90 x 12.7 cm). These dimensions are larger in lateral area and depth than the volume detected by the PGNA

system. Thus each specimen is effectively a semi-infinite slab. The volume of each slab is 3.75 ft^3. Five tiles (3ft by 3ft by 1 inch) were also cast with a total volume of 18.75 ft^3. The slabs and tiles were cast with chloride concentrations as shown in Table 5-2.

Table 5-2- Slabs Cl Content

Slab #	Cl Concentration % Cl by wt Concrete
1	0.6
2	0.5
3	0.3
4	0.025
Control	~0

Figure 5-1- A concrete slab

The chloride concentrations are selected to span the range of values typically found in the field down to the concentration that has been identified as the threshold for promoting corrosion 0.025% by weight of concrete. These slabs thus have spatially uniform concentrations of Cl,

which would be representative of a concrete mix that had calcium chloride added as an accelerator or as anti-freeze for low temperature emplacement. The PGNA model is simplified if uniform distribution is assumed. Table 5-3 illustrates the weight of each slab and their Cl_2 contents.

Table 5-3- Slabs Weight/Cl Weight

Slabs' Weight (lb)				
# 1	# 2	# 3	# 4	Control
616.056	615.520	614.440	612.968	612.816
Calcium Chloride Weight in Slabs (lb)				
# 1	# 2	# 3	# 4	Control
3.696	3.0776	1.84332	0.153242	0

5.2.2 Tiles

One shape of the concrete specimens is a tile with dimensions of 3ft by 3ft by 1 inches (90 x 90 x 2.5 cm) Figure 5-2. The volume of each tile is 0.75 ft^3. Five of these tiles were cast with a total volume of 0.75 ft^3 and with the chloride concentrations as shown in Table 5-1. The breakdown of each tile's weight and chloride weight within that specific tile is demonstrated in table 5-4.

Figure 5-2- A concrete tile

Table 5-4- Tiles Weight/Cl Weight

	Tiles Total Weight (lb)			
# 1	# 2	# 3	# 4	Control
154.014	153.880	153.610	153.242	153.204
Calcium Chloride Weight in Tiles (lb)				
# 1	# 2	# 3	# 4	Control
0.924	0.769	0.461	0.038	0.000

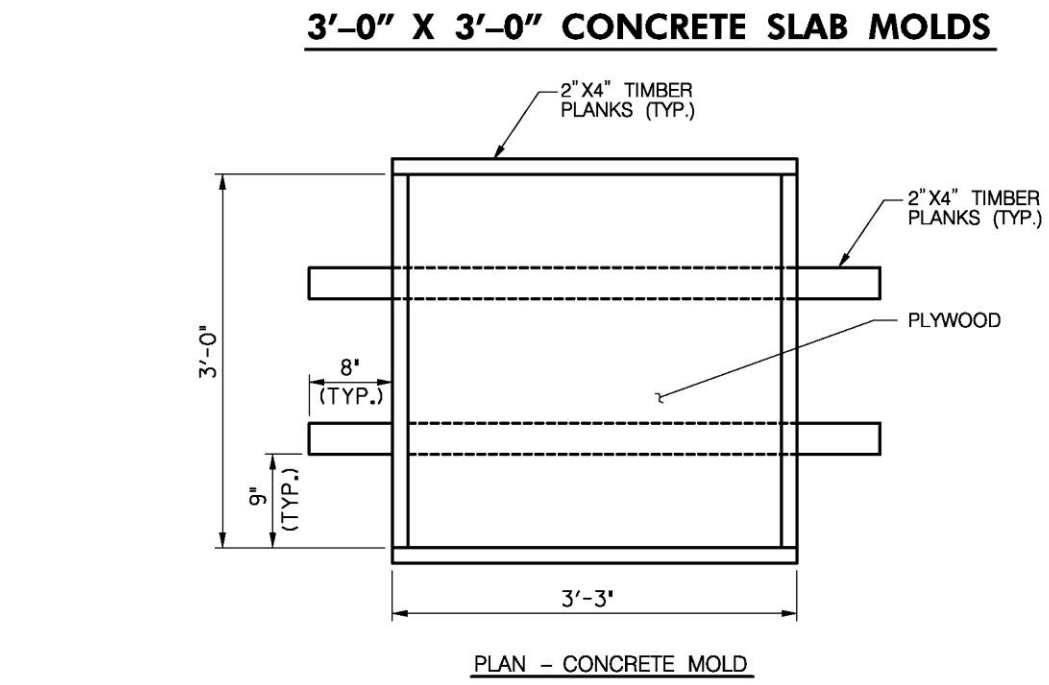

SIZE	LENGTH	QUANTITY
2"X4"	3′-0"	10
2"X4"	3′-3"	10
2"X4"	4′-7"	10
PLYWOOD	3′-3" X 3′-3"	5

TABLE 1 : 5 – 3'X3'X3" TIMBER MOLDS

Figure 5-3-Concrete slab molds

The chloride concentrations are selected to span the range of values typically found in the field down to the concentration that has been identified as the threshold for promoting corrosion which is0.025% by weight of concrete. These slabs thus have spatially uniform concentrations of chloride, which would be representative of a concrete mix that had calcium chloride added as an accelerator or as anti-freeze for low temperature emplacement.

The table below is the mix design summary that was used in casting the specimens.

Table 5-5-Concrete mix design summary

	Control	Batch # 1	Batch # 2	Batch # 3	Batch # 4
Water (lb)	65.67	65.67	65.67	65.67	65.67
Cement (lb)	131.35	131.35	131.35	131.35	131.35
Coarse Aggregate - Stone (lb)	301.00	301.00	301.00	301.00	301.00
Fine Aggerate -Sand (lb)	268.00	268.00	268.00	268.00	268.00
Calcium Chloride -$CaCl_2$ (lb)	--	4.05	3.38	2.03	0.19
Calcium Chloride -$CaCl_2$ (%) per wt. of concrete	--	0.60	0.50	0.30	0.025

The PGNA model is simplified if uniform distribution is assumed. However, the chloride content of concrete bridge decks in North America is more often the result of de-icing salts applied to the surface. This produces a non-uniform chloride depth profile which can typically be modeled as a Fick's Law-type diffusion gradient as shown Figure 5-5. This profile can take many years to develop, and thus it is difficult to prepare laboratory specimens by pounding. Therefore, to approximate this, a series of 5 thin concrete slabs each 3ft by 3ft by 1 inch (90 x 90 x 2.54 cm) were prepared. The chloride content was uniform in an individual thin slab, but it varied from slab to slab.

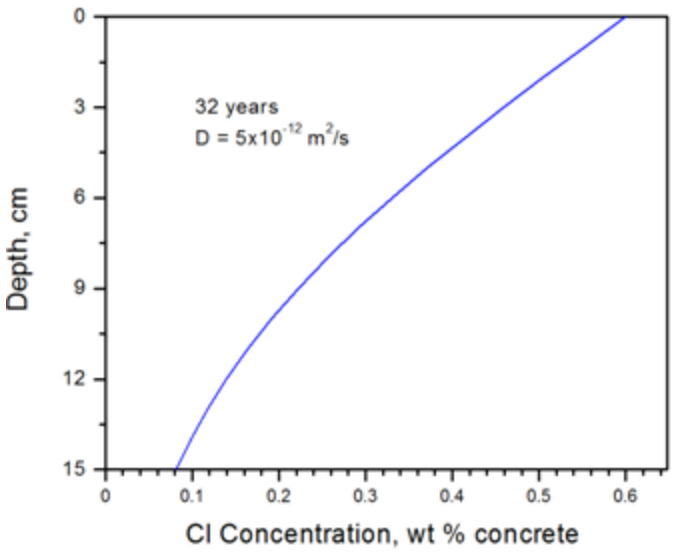

Figure 5-4-Typical Cl gradient in concrete

(Livingston, et al. (TRB), 2011)

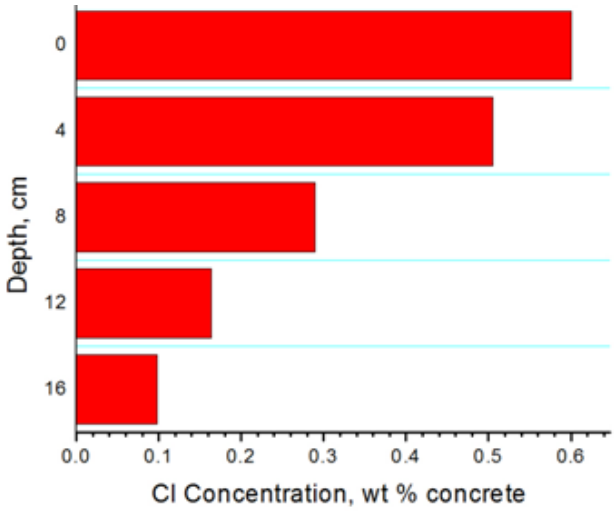

Figure 5-5-Thin concrete slab approximation to the Cl gradient in Figure 5-5

(Livingston, et al. (TRB), 2011)

5.2.3 Picture of slabs/tiles during casting

Figure 5-6- Specimens' form work

Figure 5-7- Aggregate used

Figure 5-8- Mixer

Figure 5-9- Concrete tile

Figure 5-10- Specimen's coverage

These samples are being used to determine the calibration function relating the detected Cl gamma ray counts to the actual chloride concentration in the concrete. They will also be used to determine the data quality parameters of sensitivity, precision, and minimum level of detection.

5.3 TFHRC Calibration

As previously discussed a, 2nd generation neutron-based system for the measurement of chlorides in concrete is under development with a grant from NCHRP-IDEA. A neutron source is needed in order to evaluate the detector's performance. The source for the system will be a deuterium-tritium (D-T) fusion neutron generator that is a linear accelerator emitting neutron and can be used instead of the ^{252}Cf radioisotope neutron source. However, the neutron generator is not currently available for this study. Consequently, as an initial test of the system, the existing ^{252}Cf source at TFHRC (Turner-Fairbank Highway Research Center) in Mclean Virginia was utilized.

This could not be moved to UMD because of licensing issues. Therefore, the concrete tiles were taken from UMD to TFHRC lab in order to be tested there.

The five 1" concrete tiles that were cast at UMD civil engineering lab (illustrated previously in section 5.2) were tested at TFHRC Non-Destructive Evaluation center. The PGNA system consisted only of the HPGe detector since the NaI detector was still on backorder. Thus the configuration of the system was essentially the first generation omnidirectional design.
As illustrated in Figure 5-12, the ^{252}Cf source consists of a mass of the radioisotope ^{252}Cf which is sealed in a DOT certified zircalloy-2 capsule. The^{252}Cf decays mainly by alpha emission and has a half-life of 2.7 years However, 3.1% of the decay is spontaneous fission which emits neutrons with characteristic energies around 1 MeV. The utilized quantity of ^{252}Cf was originally 10 microcuries for neutron source strength of 10^7 n/s which was decayed to about a quarter of that strength. Precautions should be taken while using ^{252}Cf and it should be stored in a proper container approved by the DOT when it is not being used (Livingston, et al., 2011).

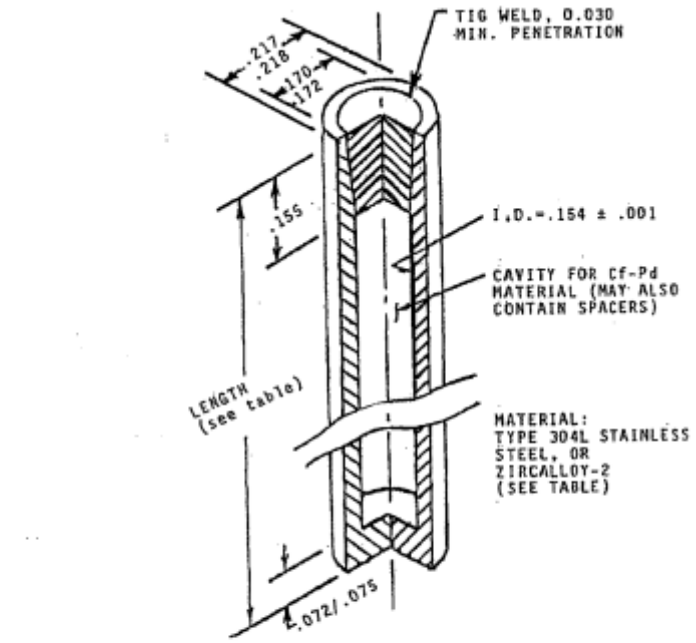

Figure 5-11- Diagram of ^{252}Cf Capsule

(Livingston, et al., 2011)

5.3.1 The Test Process

The five 1" tiles of concrete with chloride contents ranging from 0 to 0.6% by weight of concrete were tested at TFHRC NDE center. The concrete tiles were stacked in order of increasing chloride content as shown in Figure 5-13.

Figure 5-12- Stack of concrete tiles at TFHRC

A 12 feet exclusion area was marked off with a plastic chain and radiation hazard signs (Figure 5-14). A preliminary survey with the help of NIST-certified beta/gamma and neutron dose rate meters was done before the radioactive sources were brought out. A background of approximately 0.05 ± 0.025 mrem/hr was measured that was much below the occupational dose limit of 2 mrem/hr set by NRC. The PGNA system included a Canberra coaxial N-type HPGe detector which had been cooled down in advance in addition to a MCA module that was a Canberra DSA-1000. The software used for the gamma spectroscopy was Canberra Genie 2000.

The adjusted gain of the MCA that covered 10 MeV with 8192 channels gave a conversion factor of 1.22 keV per channel which was established utilizing the 1.33 MeV line of the ^{60}Co calibration source. With the aim of creating the radiation background in the lab, the first gamma-ray spectrum was done without the ^{252}Cf neutron source. The only significant peak observed in

the background spectrum was ^{40}K due to the potassium that is usually found in bricks and concrete.

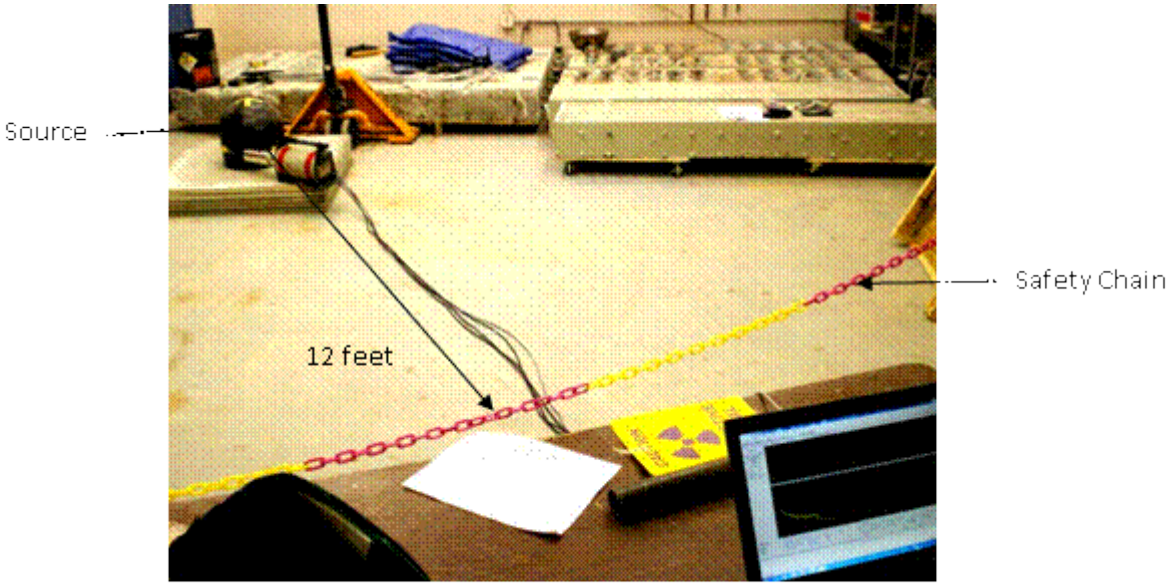

Figure 5-13- Layout of exclusion area

The neutron source which was stored in its storage cask was placed in the polyethylene moderator, which had been previously placed on the center line of the concrete slabs. The initial data acquisition which showed a dead-time of 78% was a problem since it created errors in the gamma ray counts. In order to reduce the source of radiation from PGNA which is the hydrogen in the moderator, a stack of lead bricks was placed between the moderator and the detector. As a result, the dead-time was reduced to an acceptable 7% (Livingston, et al., 2011).

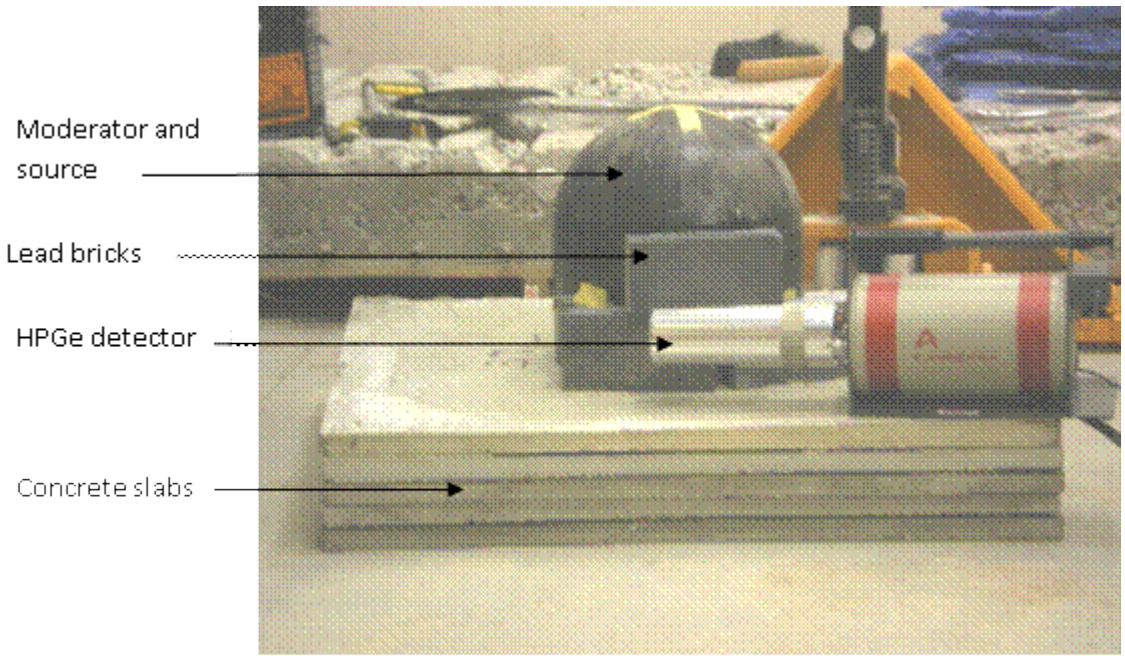

Figure 5-14-PGNA test setup

Next, a spectrum for a preset time of 1000 seconds was attained. Different projecting lines were observed such as the 2.223 MeV line for hydrogen due to the fact that hydrogen exists in the concrete in addition to in the moderator. More importantly, chlorine was successfully identified at the 6.111MeV peak along with other Chlorine lines at 5.089 and 5.598 MeV. Several other lines representing silicon were also observed since the concrete tiles were made of silicate coarse and fine aggregates. The PGNA spectrum of concrete tiles from 0 to 5 MeV and 5 to 7.5 MeV are shown in Figures 5-16 and 5-17 respectively (Livingston, et al., 2011).

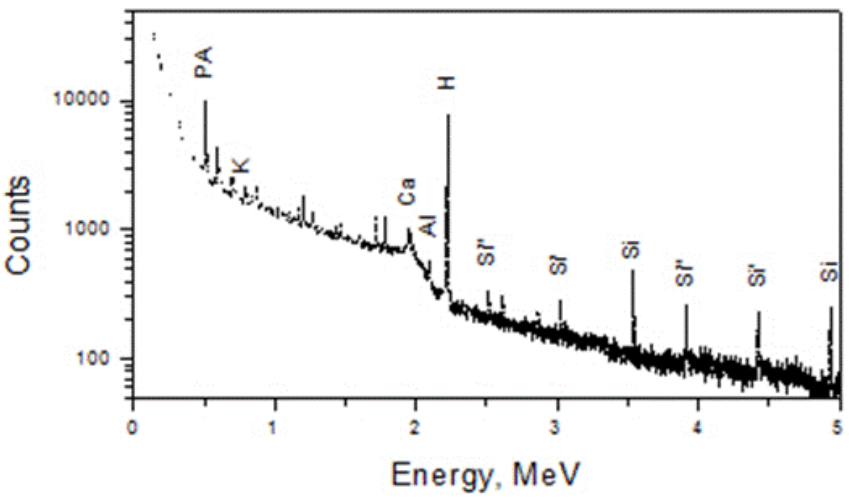

Figure 5-15- PGNA spectrum of concrete test slabs, 0-5 MeV

PA = positron annihilation peak, ′ = single escape peak; ″ = double escape peak
(Livingston, et al., 2011)

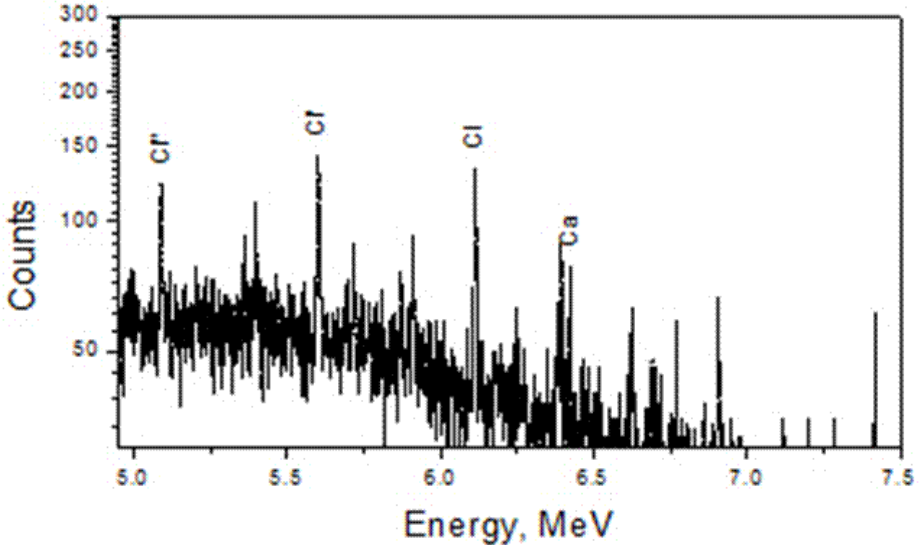

Figure 5-16- PGNA spectrum of concrete slabs, 5-7.5 MeV

PA = positron annihilation peak, ′ = single escape peak; ″ = double escape peak
(Livingston, et al., 2011)

Defining the region of interest for the peak, Chlorine 6.111 MeV peak was analyzed manually which ranged between the 6.014 and 6.120 MeV channels (Figure5-18).

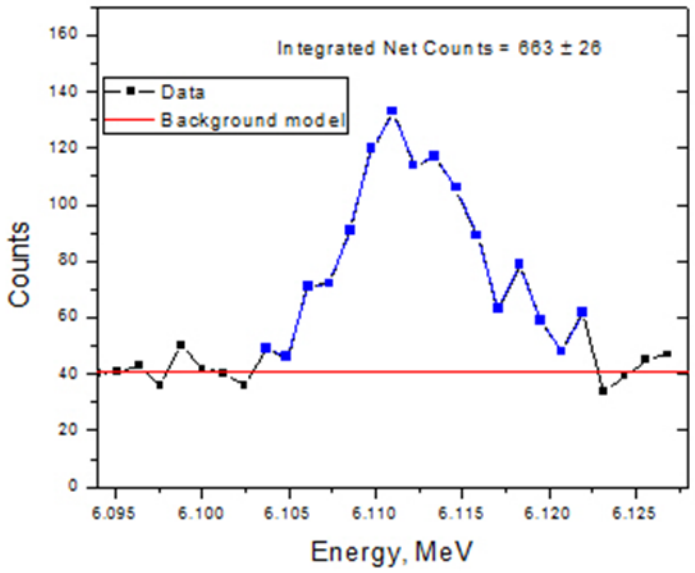

Figure 5-17-The 6.111 MeV chlorine peak in the PGNA spectrum

(Livingston, et al., 2011)

5.3.2 Interpretation of Results

The background was modeled using a number of different channels on either sides of the peak. A constant horizontal flat background model was found suitable as shown by the red line which had the average background of 41 counts per channel (Figure 5-18). In order to find the net count that represents the gamma rays due to Chlorine, this number was subtracted from each of the channels in the 6.111 MeV peak. The net counts were then integrated over all the channels in the peak to give the area of the peak, which is the total Chlorine signal. As a result, a 663 ± 26 counts or an uncertainty of 4% was attained (Livingston, et al., 2011).

The number of counts divided by the counting time (1000 second in this study) is defined as count rate. In this study the count rate was 0.663 cps, which is a little low due to the fact that the ^{252}Cf source was weak since it had been decayed to about a quarter of its original strength. In general, 1 cps or more is preferred.

The objective of this experiment was to obtain the calibration factor which is the chloride weight in percent divided by number of counts. However, this could not be achieved very precisely since this experiment was done on a stack of thin concrete tiles (1 Inch depth- see Figure 5-13) with varying chloride contents. The fraction of the total measured gamma ray signal contribured each of the slabs is difficult to calculate analytically because of the complications of neutron and gamma transport. However, a rough idea of the calibration factor can be obtained by assuming that most of the signal came from the top three slabs, which had Cl concentrations ranging between 0.3-0.6 %. Using a representative value of 0.5% Cl, the calibration factor is 0.663 cps /0.5% Cl = 1.33 cps/%Cl with an uncertainty of at least 10%. This is essentially the sensitivity of the system. The implication is that for a chloride concentration at the corrosion threshold level of 0.025%, the count rate would be 0.033 cps. Assuming that this could be detected in the presence of the background noise, it would take 30,300 seconds of counting to obtain 1000 counts, or 8.4 hours. This would be too slow for field use. However, the low count rate is a direct result of the weak ^{252}Cf neutron source used in this experiment. The neutron source planned for the 2nd generation detector would have a strength at least an order of magnitude greater. Since the measurements were made on only a single concentration of chloride, it is not possible to estimate the other data quality parameters such as minimum level of detection.

6 CHAPTER SIX: SUMMARY AND CONCLUSIONS

6.1 Summary

A major cause of the deterioration of reinforced concrete structures is corrosion and deterioration promoted by chlorides from road de-icing salts. The real hazard of this deterioration is illustrated by the collapse of a highway overpass in Laval, Quebec that killed 5 people and injured 6 others. The official report of the Commission of Inquiry concluded that a major factor in the collapse was concrete deterioration due to de-icing salts. Therefore, there is a critical need for a nondestructive test method that can detect chlorides in concrete to measure nondestructively the condition of existing masonry or reinforced concrete structures, particularly behind surface finishes. The PGNA based method can help to meet this need (Livingston, et al.(TRB), 2010).

This method has the advantage over other types of nondestructive methods, since it can measure the chemical composition present in the concrete rather than structural or mechanical aspects. This technique works by irradiating neutrons from a portable neutron source to a small piece of concrete. Then characteristic gamma rays are produced by neutrons passing through the concrete; and these gamma rays will be identified and counted at the end. The collected data from the sample is read in order to gather the information regarding the spatial distribution of characteristic elements. PGNA can be utilized to identify several features of concrete position and conditions such as detecting the amount of chloride in the structure. Chloride detection is the most significant usage of PGNA in reinforced concrete structures. This process can be easily done due to the fact that chlorine cross section can capture a very large thermal neutron (Livingston, et al.(TRB), 2010).

6.2 Conclusions

Corrosion of reinforcement in bridge decks is a major problem for United States infrastructure. A rapid, non-destructive, spatially resolved, and objective inspection tool for detecting corrosion of reinforcement in concrete at an early stage could lead to planning reliability and a saving of billions of US-Dollars in the public and private budgets. Deicing salt such as calcium chloride is the main cause of corrosion in reinforced bridge decks. The current technique of measuring chloride content in concrete, AASHTO T 260-94, is destructive and time-consuming
A nondestructive method the first generation PGNA was an improved version which is omni-directional and can test a large volume which needed improvements. In order to overcome the spatial resolution and make the detector more directional, in the second generation PGNA a collimator to constrain the solid angle in which the gamma-rays are detected was introduced. The need for a nondestructive method that can measure and monitor the chloride content in bridge decks can be met by using second generation PGNA. Most of the existing methods are destructive and require intense labor and consume a lot of time. Utilizing PGNA method can help control, measure, and monitor the quantity of chloride content in structures and it can improve the rehabilitation of our bridges across the nation.

REFERENCES

Angst, U., & Venbesland, O. (2009). Critical chloride content in reinforced concrete. State of the art. *Concrete repair, rehabilitation and retrofitting II, Capetown,* South Africa.

Cady, P., & Gannon, E. (1992). Condition evaluation of concrete bridges relative to reinforcement corrosion. *SHRP, 1*, 1-75.

Clear, K., & Hay, R. (1973). Time to corrosion of reinforcing steel in concrete slabs. *(Report No.FHWA-RD-73-32),Federal Highway Administration, 1*, 1-103.

Goldmark, A. (2011, March 30). One in nine bridges in America â€œStructurally Deficient, Potentially Dangerousâ€ • . *Transportation Nation, 1*, 1. Retrieved April 15, 2011, from Transportation.org

Huston, D., Fuhr, P., Maser, K., & Weedon, W. (2002). Nondestructive testing of reinforced concrete bridges using Radar Imaging Techniques. *Department of Mechanical Engineering College of Engineering & Mathematics University of Vermont Burlington, VT, NETCR 94-2*, 16-18.

Jang, S. B., Lee, C. S., & Oh, B. H. (2004). Chloride diffusion and corrosion initiation time of reinforced concrete structures. *International workshop on micro-structure and durability to predict service life of concrete structures, 1*, 5-6.

Laferriere, F., Pascal, P. K., Inaudi, D., & Smith, I. F. (2008). A new system for early chloride detection in concrete. *Smart Materials and Structures, 17*(4), 587-600.

Livingston, R.A, Al-Sheikhly, M., & Mohamed, A.B. (2010). Numerical simulation of the PGNA signal from chlorine diffusion gradients in concrete. *Applied Radiation and*

Isotopes, *68*(4-5), 670-682.

Livingston, R. A., Al-Sheikhly, M., & Amde, A. (2011). Second generation neutron-based system for measuring chlorides in concrete . *The Transportation Research Board (TRB) 90th Annual Conference, Washington, D.C*, January 23-27.

Livingston, R., Amde, A. M., Bozorgi, N., Hicks, P. D., & Mangle, J. H. (2011). *Summary of PGNA measurements at Turner Fairbank Highway Research Center*.

Livingston, R. A. (1993). Applied Radiation and Isotopes. *Standardization of the neutron probe for the assessment of masonry deterioration*, *44*(10-11), 1285-1300.

Livingston, R. A., & Saleh, H. (2000). Experimental evaluation of a portable neutron-based gamma spectroscopy system for chloride measurements in reinforced concrete. *Journal of Radioanalytical and Nuclear Chemistry*, *244*(2), 367-371.

Manning, D., & Masliwec, T. (1990). Operational experience using Radar and Thermography for bridge deck condition survey. *NDE of Civ. Struc. and Mater, Boulder (CO)*, 233-234.

Pradhan, B., & Bhattacharjee, B. (2009). Half-cell potential as an indicator of chloride-induced rebar corrosion initiation in RC. *Journal of Materials in Civil Engineering*, *21*(10), 542-552.

Rhazi, J. (2001). The case of concrete bridge deck. *NDT in Civil Engineering*, *6*(5). Retrieved April 10, 2011, from www.NDT.net

Song, H., & Saraswathy, V. (2007). Corrosion monitoring of reinforced concrete structures. *International Journal of Electrochemical Science*, *2*, 1-27.

Tonini, D., & Dean, S. (1977). Chloride corrosion of steel in concrete. *ASTM, STP 629*, 3-10.

Weyers, R. E., Kirkpatrick, T. J., Anderson-Cook, C. M., & Sprinkel, M. M. (2002).

Probabilistic model for the chloride-induced corrosion. *Cement and Concrete Research, 32*(12), 1943-1960 .